

Steric Hindrance as a Mechanistic Probe for Olefin Reactivity: Variability of the Hydrogenic Canopy over the Isomeric Adamantylideneadamantane/Sesquihomoadamantene Pair (A Combined Experimental and Theoretical Study)

R. Rathore, S. V. Lindeman, C.-J. Zhu, T. Mori, P. v. R. Schleyer,[†] and J. K. Kochi*

Departments of Chemistry, University of Houston, Houston, Texas 77204-5003, and University of Georgia, Athens, Georgia 30602-2556

jkochi@mail.uh.edu

Received January 30, 2002

Access to each C=C face of adamantylideneadamantane (**AA**) and sesquihomoadamantene (**SA**) is hindered by the hydrogenic canopy consisting of four β -hydrogens; otherwise, these olefins have quite normal environments. X-ray crystallography and density functional (DFT) calculations show a 0.5 Å larger annular opening in the protective cover of **AA** than that in **SA**. This contributes to the remarkable differences in reactivity toward various reagents, not only by limiting access to the olefin site in **SA** but also by inhibiting reactions which force these hydrogens closer together. Thus, **AA** is subject to typical olefin-addition reactions with bromine, sulfonyl chloride, *m*-chloroperbenzoic acid, dioxygen, and so forth, albeit sometimes at attenuated rates. On the other hand, **SA** is singularly unreactive under identical reaction conditions, except for the notable exceptions that include Brønsted (protonic) acids, a nitrosonium cation, and dichlorine. The exceptions are characterized as three sterically limited (electrophilic) reagents whose unique reactivity patterns are shown to be strongly influenced by steric access to the C=C center. As such, the different degrees of steric encumbrance in the isomeric donors **AA** and **SA** shed considerable light on the diverse nature of olefinic reactions. In particular, they evoke mechanistic features in electrophilic addition versus electron transfer, which are otherwise not readily discernible with other less hindered olefinic donors. Transient structures of the olefinic-reaction intermediates such as the protonated carbocations **AA**-H⁺ and **SA**-H⁺ as well as the cation radicals **AA**^{•+} and **SA**^{•+} are probed by the combination of X-ray crystallographic analyses and density functional theoretical computations.

Introduction

Dual reactivity of olefinic donors is known by their susceptibility to different electrophiles, such as Brønsted and Lewis acids, chlorine, bromine, and so forth,^{1,2} as well as various inorganic oxidants, such as permanganate, nitrosonium, ferric and cupric salts, and so forth.^{3,4} Electrophilic reactivity is commonly considered to involve a two-electron process via a diamagnetic (carbocationic) intermediate,⁵ whereas olefin oxidations can be stepwise

(one-electron) processes and involve paramagnetic (cation-radical) intermediates.⁶ However, it is also possible that an electrophilic reaction of an olefin may actually proceed via two successive electron-transfer steps.⁷ In this mechanistic situation, an olefin cation radical is the viable intermediate, although it may not be experimentally detected, owing to a fast subsequent (follow-up) step.

We recently compared olefin reactivities under both electrophilic and electron-transfer perturbations and came to the conclusion that the two mechanistic pathways are very difficult to differentiate.⁸ Since steric hindrance has been successfully employed to distinguish concerted and stepwise mechanisms, we sought a sterically encumbered olefin to test the viability of the electron-transfer mechanism in some typical electrophilic reactions. Indeed, stepwise and concerted processes have been clearly delineated by Brown and co-workers in bromine addition to the quasi-hindered adamantylide-

[†] University of Georgia.

(1) (a) Olah, G. A.; Schilling, P.; Westerman, P. W.; Lin, H. C. *J. Am. Chem. Soc.* **1974**, *96*, 3581. (b) Schmid, G. H. In *The Chemistry of Double-Bonded Functional Groups*; Patai, S., Ed.; Wiley: New York, 1989. (c) Banthorpe, D. V. *Chem. Rev.* **1970**, *70*, 295.

(2) (a) Strating, H.; Wieringa, J. H.; Wynberg, H. *J. Chem. Soc., Chem. Commun.* **1969**, 907. (b) Ruasse, M. F. *Adv. Phys. Org. Chem.* **1993**, *28*, 207. (c) Fukuzumi, S.; Kochi, J. K. *J. Am. Chem. Soc.* **1982**, *104*, 7599.

(3) (a) Lee, D. G.; Chen, T. In *Comprehensive Organic Synthesis*; Trost, B. M.; Fleming, I., Eds.; Pergamon: New York, 1991; Vol. 7, p 541. (b) Bosch, E.; Kochi, J. K. *J. Chem. Commun.* **1993**, 667. (c) Bosch, E.; Kochi, J. K. *Res. Chem. Intermed.* **1996**, *22*, 209.

(4) (a) Murray, R. W. *Chem. Rev.* **1989**, *89*, 1187. (b) Koevner, T.; Slebocka-Tilt, H.; Brown, R. S. *J. Org. Chem.* **1999**, *64*, 196. (c) Ando, W., Ed. *Organic Peroxides*; Wiley: New York, 1992.

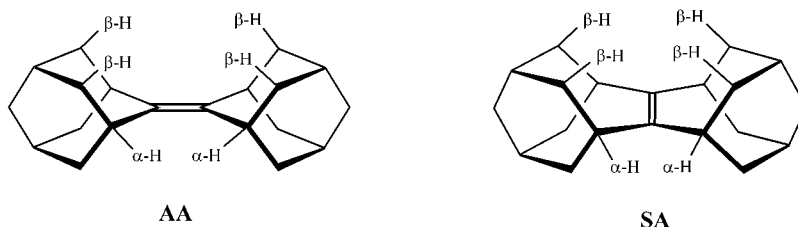
(5) (a) Olah, G. A. *J. Am. Chem. Soc.* **1972**, *94*, 808. (b) de la Mare, P. B. D.; Bolton, R. *Electrophilic Additions to Unsaturated Systems*; Elsevier: Amsterdam, 1966.

(6) (a) Rathore, R.; Kochi, J. K. *Adv. Phys. Org. Chem.* **2000**, *35*, 193. (b) Fukuzumi, S.; Kochi, J. K. *J. Am. Chem. Soc.* **1981**, *103*, 7240. (c) Lee, D. G.; Spitzer, U. A. *J. Org. Chem.* **1976**, *41*, 3644.

(7) (a) Bockman, T. M.; Kochi, J. K. *J. Phys. Org. Chem.* **1994**, *7*, 325. (b) Kochi, J. K. In *Comprehensive Organic Syntheses*; Trost, B. M.; Fleming, I.; Ley, S. V., Eds.; Pergamon: New York, 1981; Vol. 7, p 849 ff.

(8) Rathore, R.; Kochi, J. K. *Acta Chem. Scand.* **1998**, *53*, 114.

CHART 1

TABLE 1. Molecular Structures of AA and SA by X-ray Crystallography^a and Theoretical (DFT) Calculations

	X-ray	B3LYP/6-31G* ^{b,c}	difference [X-ray – DFT]	X-ray	B3LYP/6-31G* ^{b,d}	difference [X-ray – DFT]
<i>l</i> (Å)	1.344	1.350	–0.006	1.346	1.345	0.001
<i>a</i> (Å)	1.523	1.528	–0.005	1.527	1.534	–0.007
<i>b</i> (Å)	1.545	1.550	–0.005	1.544	1.551	–0.007
<i>c</i> (Å)	1.534	1.541	–0.007	1.535	1.541	–0.006
<i>d</i> (Å)	1.541	1.544	–0.003	1.534	1.540	–0.006
<i>r</i> ^e (Å)	2.00	2.10	–0.10	1.55	1.60	–0.05
<i>φ</i> (deg)	0.0	0.0		0.0	0.0	

^a Corrected for thermal motion. ^b Minimum in D_{2h} symmetry. ^c Energy, 779.018 32 au; zero point energy, 279.75 kcal/mol (unscaled). ^d Energy, 779.001 92 au; zero point energy, 280.12 kcal/mol. ^e The van der Waals cross section of the annular opening as determined by subtracting 2.4 Å (twice the hydrogen van der Waals radius) from the diagonal distances between the subtended β and β' hydrogens.

neadamantane (AA).⁹ Thus, our starting point is to focus on AA and its closely related isomer sesquihomoadamantene (SA),¹⁰ where the steric hindrance due to the rigid (cage) structure (see Chart 1) is even greater.¹¹

In this study, the contrasting behaviors of these isomeric olefins are considered in the light of subtle differences in the steric properties of AA and SA and the molecular structures of their cation radicals. Thus, the availability of single crystals of AA and SA allows the experimental examination of their cage structures (by low-temperature X-ray crystallography) that are congruent with those given by density functional theoretical (DFT) calculations. This success is also applied to the structure of the open-shell cation radical $SA^{+\bullet}$, recently determined by X-ray crystallography,¹² and to $AA^{+\bullet}$ which is too transient to isolate. Numerous species too transient to characterize have also been computed with DFT, and their energies have been evaluated.

Results

I. Steric Hindrance in the Olefinic Donors AA and SA. High quality single (colorless) crystals of AA and SA (synthesized by literature methods¹⁰ and purified by chromatography on silica gel; see Experimental Section) were obtained by careful crystallization from diethyl ether at $-30\text{ }^{\circ}\text{C}$. X-ray crystallographic data were collected at $-150\text{ }^{\circ}\text{C}$ and to relatively high diffraction angles ($\sin \theta/\lambda \leq 0.8$) so that the precision of the pertinent bond distances in Table 1 is $\pm 0.1\text{ pm}$ and that of the bond angles is $\pm 0.05^{\circ}$.¹³

The molecular structures of adamantylideneadamantane and sesquihomoadamantene calculated by density functional theory (DFT) at the B3LYP/6-31G* level are included in Table 1 for comparison. The agreement between the experimental and theoretical structures of AA and SA is given by the numbers in columns 4 and 7 of Table 1.

The carbon–carbon double bonds in both AA and SA have normal bond lengths and are precisely planar; the rigid cage structures ensure minimal conformational distortions. The C–C bond distances and bond angles in AA are those expected for an essentially strain-free olefin, but SA has the modest strain associated with the seven-membered rings, causing a slight contraction of the C=C–C ring angles. In agreement, the DFT computations find both AA and SA to be energy minima in D_{2h} symmetry; SA is 10.7 kcal/mol less stable than AA when corrections for the zero-point energies are included.

(9) (a) Brown, R. S. *Acc. Chem. Res.* **1997**, *30*, 131. (b) See also: Chiappe, C.; Rubertis, A. de; Lemmon, P.; Lenoir, D. *J. Org. Chem.* **2000**, *65*, 1273.

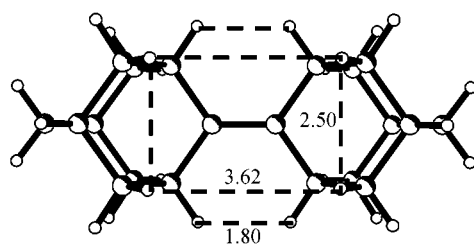
(10) (a) Wynberg, H.; Boelema, E.; Wieringa, J. H.; Strating, J. *Tetrahedron Lett.* **1970**, 3613. (b) Boelema, E.; Wynberg, H.; Strating, J. *Tetrahedron Lett.* **1971**, 4029.

(11) (a) SA was previously identified as a “hyperstable” olefin, since the strain of the hydrogenated product (SAH_2) was computed to be about 13 kcal/mol greater than that of SA.^{11b} Because of the greater flexibility of its hydrogenated product (AAH_2), AA does not exhibit this problem, and its driving force toward saturation reactions is not reduced. On this basis, SA was also predicted to be less reactive than AA. (b) McEwen, A. B.; Schleyer, P. v. R. *J. Am. Chem. Soc.* **1986**, *108*, 3951. (c) The B3LYP/6-31G* value is nearly identical to the MM2 result. AA does not exhibit this problem, since its hydrogenated product AAH_2 can twist to avoid crowding. Thus, it is approximately 10 kcal/mol more difficult to “saturate” the double bond in SA than AA. This comparison is shown directly by the following equality: $AAH_2(C_{2h}) + SA = SAH_2(C_{2h}) + AA + 9.88\text{ kcal/mol}$.

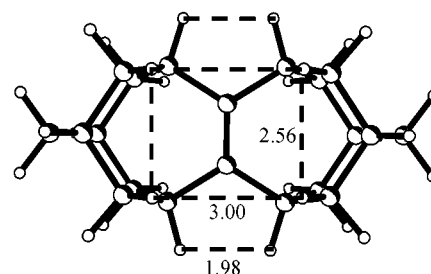
(12) Rathore, R.; Zhu, C.-J.; Lindeman, S. V.; Kochi, J. K. *Angew. Chem., Int. Ed. Engl.* **2000**, *42*, 3817.

(13) For the less precise X-ray structures at room temperature, see the following. (a) SA: Watson, W. H.; Nagl, A. *Acta Crystallogr.* **1987**, *C43*, 2465. (b) AA: Swen-Walstra, S. C.; Visser, G. J. *J. Chem. Soc. D* **1971**, 82.

CHART 2



AA



SA

Most importantly, steric hindrance is imposed by virtue of a set of four β -protons lying directly over each face of the double bonds (Chart 1). In **AA**, the protective cover of four β -protons forms a rectangular array so that the nearest (nonbonded) neighbors are separated by 2.50 Å (β, β) and 3.62 Å (β, β'), as illustrated in the left perspective in Chart 2.

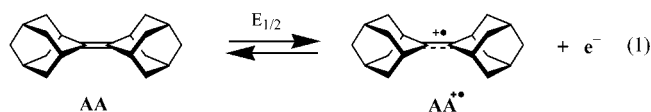
DFT computations lead to essentially the same separations of 2.61 Å (β, β) and 3.66 Å (β, β'). Moreover, the α -protons lying in the equatorial (C=C) plane are in closer van der Waals contact; the α, α' separations are 1.85 and 1.89 Å (DFT).

By way of contrast, in **SA** the four β -protons describe a slightly elongated square; the 2.56 Å (β, β) and 3.00 Å (β, β') distances are more nearly equal, and the corresponding DFT separations are 2.61 and 3.02 Å, respectively. The α -protons in **SA** are separated by greater distances [1.98 and 2.00 Å (DFT)] than they are in the isomeric **AA**.

On the basis of the X-ray crystallographic as well as the DFT calculations, we conclude that the steric access to the double bond in **AA** is limited to a van der Waals annular opening of 2.0 Å diameter, whereas in **SA** it is significantly less (1.5 Å).¹⁴ Otherwise, there is basically minimal difference in the overall structural morphology between **AA** and **SA**.

II. Electron-Donor Properties of the Olefinic Donors AA and SA. Olefin reactivity can be conveniently evaluated according to its electron-donor properties, as quantitatively judged by the reversible oxidation potential (E°_{ox}) in solution.^{7b,15} To this end, we found the electrochemical oxidation of 5.0 mM adamantylideneadamantane (**AA**) in anhydrous dichloromethane (containing 0.2 M tetra-*n*-butylammonium hexafluorophosphate) to show a reversible cyclic voltammogram with a cathodic/anodic peak current ratio of $i_a/i_c = 1.0$ (theoreti-

cal) at a scan rate of $\nu = 100 \text{ mV s}^{-1}$. Calibration of the peak currents with ferrocene provided the reversible oxidation potential $E_{1/2} = 1.46 \text{ V}$ versus SCE which compares with 1.45 V originally measured by Nelsen and co-workers^{15a} for the reversible production of the **AA** cation radical.



The isomeric sesquihomoadamantene (**SA**) underwent the same reversible electrochemical oxidation at a similar reversible potential of $E_{1/2} = 1.34 \text{ V}$ versus SCE. The difference in these E°_{ox} evaluations of 0.12 mV (which agrees with Nelsen's^{34b} 2.8 kcal/mol difference and with the computed gas phase difference of 2.3 kcal/mol) confirms that the donor strengths of **AA** and **SA** are thermodynamically rather similar.

The most pronounced difference between **AA** and **SA** as olefinic donors lies in the lifetimes of the cation-radical products **AA**^{•+} and **SA**^{•+}. For example, the bulk electrolysis of sesquihomoadamantene (**SA**) at an anodic potential of $E = 1.3 \text{ V}$ produced the dark purple solution of **SA**^{•+} in dichloromethane from which the pure salt **SA**^{•+}PF₆⁻ could be isolated in high yields. In marked contrast, the isolation of the cation radical of adamantylideneadamantane (via bulk electrolysis under the same conditions) was singularly unsuccessful, owing to the rapid decomposition of **AA**^{•+} even at -78°C . Indeed, the metastable character of **AA**^{•+} in anodic oxidation coincides with previous oxidation studies of adamantylideneadamantane by Nelsen and co-workers^{15,34b} from which its intrinsic lifetime can be estimated as $<5 \text{ s}$.¹⁶

III. Chemical Oxidation of the Olefinic Donors AA and SA. The chemical (one-electron) oxidation of

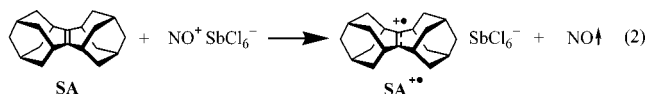
(14) (a) Calculated by subtraction of twice the van der Waals radius of hydrogen (2.4 Å) from the corresponding diagonal distance between β and β' hydrogens. (b) It is important to emphasize that the experimental values of bond distances/angles determined by X-ray crystallography differ slightly from those obtained via computation by amounts relating to molecular thermal motion. (c) The hydrogen locations were based on the "neutronographic" values 1.1 Å along the electron-density vectors established by X-ray crystallography at each carbon center.

(15) (a) Nelsen, S. F.; Kapp, D. L.; Akaba, R.; Evans, D. H. *J. Am. Chem. Soc.* **1986**, *108*, 6863. (b) Nelsen, S. F.; Kessel, C. R. *J. Am. Chem. Soc.* **1979**, *101*, 2503. (c) Clark, T.; Teasley, M. F.; Nelsen, S. F.; Wynberg, H. *J. Am. Chem. Soc.* **1987**, *109*, 5719. (d) Gerson, F.; Gescheidt, G.; Nelsen, S. F.; Paquette, L. A.; Teasley, M. F.; Waykole, L. *J. Am. Chem. Soc.* **1989**, *111*, 5518. (e) Nelsen and co-workers first reported the transient (UV-vis) absorption spectrum of **AA**^{•+} [$\lambda_{\text{max}} = 525$ and 340 nm (sh)].^{15c}

(16) (a) Instability of such olefin cation radicals usually derives from the lability of α -protons to yield the corresponding allylic radicals. However, in **AA**^{•+}, the C-H $_{\alpha}$ bond is orthogonal to the π -orbital and renders these protons less labile. A study is underway to isolate the product(s) of decomposition. (b) Although hydrocarbon radical cations can rearrange quite readily when further unsaturation is present, an **AA**^{•+} \rightarrow **SA**^{•+} interconversion does not appear to be feasible. The B3LYP/6-31G* barrier 50.8 kcal/mol for the degenerate rearrangement of the model tetramethylethylene radical cation is too high. The transition state (CH₃)₃C-C^{•+}-CH₃ (a carbyne radical cation with a "five-electron" carbon) is very unfavorable energetically. Moreover, the energy of the less persistent **AA**^{•+} isomer is computed (B3LYP/6-31G*) to be 9.6 kcal/mol lower than that of the isolable **SA**^{•+}. (c) Olah et al.^{1a} reported the NMR observation of cationic σ -bonded intermediates and a "clear solution" from the reaction of **AA** with NO⁺BF₆⁻ at -70°C in the more polar solvent, liquid SO₂.

olefinic and related donors is conveniently effected by nitrosonium (NO^+), owing to its reversible reduction potential $E^\circ_{\text{ox}} = 1.48 \text{ V}$ in dichloromethane. The removal of the gaseous reduction product (NO) ensures a chemically irreversible oxidation.

A solution of the sesquihomoadamantene (**SA**) in dichloromethane was added to the crystalline salt $\text{NO}^+\text{SbCl}_6^-$ (under an argon atmosphere) at $\sim -78^\circ\text{C}$. Continued stirring and removal of nitric oxide (by bubbling argon through the dark solution) afforded a bright purple solution (see Experimental Section). Spectral (UV-vis) analysis of the deep purple solution showed a characteristic absorption spectrum with absorption bands at $\lambda_{\text{max}} = 360$ ($\epsilon_{360} = 4000 \pm 200 \text{ M}^{-1} \text{ cm}^{-1}$) and 485 nm , as reported by Nelsen and co-workers^{15c} for the quantitative formation of $\text{SA}^{+\bullet}$ which was determined spectrophotometrically, that is,



(Note that the absorption spectrum of the $\text{SA}^{+\bullet}$ cation radical was identical to that obtained above by electrochemical oxidation in dichloromethane.) The purple salt was isolated as a microcrystalline powder by slow diffusion of toluene into the dichloromethane solution of $\text{SA}^{+\bullet}\text{SbCl}_6^-$ at -78°C ; it could be quantitatively reduced back to the neutral donor with iodide, that is,

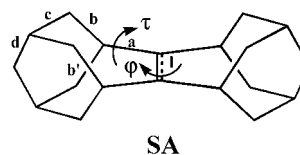


The titration of the liberated iodine with aqueous thio-sulfate indicated the purity of the isolated $\text{SA}^{+\bullet}\text{SbCl}_6^-$ to be greater than 98%. Most importantly, the extraction of the aqueous layer with diethyl ether after iodide reduction (followed by chromatographic purification) led to the recovery of the neutral sesquihomoadamantene (**SA**) in essentially quantitative yield.

Oxidation of adamantylideneadamantane (**AA**) was also readily effected with nitrosonium hexachloroantimonate under the same conditions, although we were unable to directly observe $\text{AA}^{+\bullet}$ cation radical, as judged by repeated spectral examinations.^{16c} Indeed, our inability to isolate any free olefin from the reaction mixtures (after iodide reduction) accords with the rapid (and irreversible) decomposition of $\text{AA}^{+\bullet}$ observed in bulk electrolysis (vide supra).

IV. Molecular Structures of the Olefinic Cation Radicals $\text{SA}^{+\bullet}$ and $\text{AA}^{+\bullet}$. The cation-radical salt $\text{SA}^{+\bullet}\text{SbCl}_6^-$ was recrystallized and successfully isolated as dark purple crystals by the slow diffusion of hexane into a dilute (dichloromethane) solution at -50°C . Single-crystal analysis by X-ray crystallography at -150°C (Table 2) clearly establishes a 29° twist of the central olefinic bond in $\text{SA}^{+\bullet}$ compared to that in the planar (neutral) donor **SA** itself, as predicted theoretically.^{17–21} A careful comparison of the X-ray structure of the

TABLE 2. Comparison of the Principal Geometrical Parameters^a of the Cation Radical $\text{SA}^{+\bullet}$, as Evaluated by X-ray Crystallography and Theoretical (DFT) Calculations



	$\text{SA}^{+\bullet}$			$\text{AA}^{+\bullet}$
	X-ray	B3LYP/6-31G*	difference [X-ray – DFT]	B3LYP/6-31G*
l (Å)	1.397(3)	1.411	–0.014	1.418
a (Å)	1.491(3)	1.501	–0.010	1.496
b (Å)	1.558(3)	1.571	–0.013	1.566
b' (Å)	1.541(3)	1.556	–0.015	1.568
c (Å)	1.530(3)	1.537	–0.007	1.536
d (Å)	1.529(3)	1.539	–0.010	1.543
α^a (deg)	108.1(2)	109.4	–1.3	108.6
α'^a (deg)	115.2(2)	114.9	+0.3	108.9
φ (deg)	29.0(2)	24.1	+4.3	20.9
τ^b (deg)	82.3(2)	79.2	+3.1	+121.2
τ'^b (deg)	–43.1(2)	–46.5	–3.4	–121.1

^a α and α' are angles between bonds ab and ab' , respectively. ^b τ and τ' are dihedral angles between planes determined by bonds la/ab and la/ab' , respectively.

sesquihomoadamantene cation radical with the molecular structure obtained by theoretical calculations at the B3LYP/6-31G* level²² is summarized in Table 2. It is noteworthy that the X-ray and theoretical structures of $\text{SA}^{+\bullet}$ by and large yield bond distances and bond angles that are coincident to within 1 pm and 1° , respectively.^{14b} The dihedral angles were reproduced with slightly less reliability, but the pronounced twist about the central (olefin) bond of $\varphi = 29.0 \pm 0.2^\circ$ was unmistakable.

The transient character of the cation radical from adamantylideneadamantane ($\text{AA}^{+\bullet}$) precluded the isolation of a crystalline salt for X-ray analysis. Hence, we relied on the B3LYP/6-31G* optimized geometry of $\text{AA}^{+\bullet}$, since the validity of such open-shell computations was established for $\text{SA}^{+\bullet}$. Indeed, the calculated bond lengths and bond angles in $\text{AA}^{+\bullet}$ are similar to those established for the isomeric $\text{SA}^{+\bullet}$ in Table 2.

The changes in molecular structure accompanying the oxidation of olefin donors to their cation radicals are

(19) (a) Merer, A. J.; Schoonveld, L. *J. Chem. Phys.* **1968**, *48*, 522. (b) Merer, A. J.; Schoonveld, L. *Can. J. Phys.* **1969**, *47*, 1731.

(20) Koppel, H.; Domcke, W.; Cederbaum, L. S.; Niessen, W. V. *J. Chem. Phys.* **1978**, *69*, 4252.

(21) (a) Toriyama, K.; Okazaki, M. *Appl. Magn. Reson.* **1996**, *11*, 47 and references therein. (b) Shiotani, K.; Nagata, Y.; Sohma, J. *J. Am. Chem. Soc.* **1984**, *106*, 4640.

(22) (a) Frisch, M. J.; Trucks, G. W.; Schlegel, H. B.; Scuseria, G. E.; Robb, M. A.; Cheeseman, J. R.; Zakrzewski, V. G.; Montgomery, J. A., Jr.; Stratmann, R. E.; Burant, J. C.; Dapprich, S.; Millan, J. M.; Daniels, A. D.; Kudin, K. N.; Strain, M. C.; Farkas, O.; Tomasi, J.; Barone, V.; Cossi, M.; Cammi, R.; Mennucci, B.; Pomelli, C.; Adamo, C.; Clifford, S.; Ochterski, J.; Petersson, G. A.; Ayala, P. Y.; Cui, Q.; Morokuma, K.; Malick, D. K.; Rabuck, A. D.; Raghavachari, K.; Foresman, J. B.; Cioslowski, J.; Ortiz, J. V.; Stefanov, B. B.; Liu, G.; Liashenko, A.; Piskorz, P.; Komaroni, I.; Gomperts, R.; Martin, R. L.; Fox, D. J.; Keith, T.; Al-Laham, M. A.; Peng, C. Y.; Nanayakkara, A.; González, C.; Challacombe, M.; Gill, P. M. W.; Johnson, B.; Chen, W.; Replogle, E. S.; Pople, J. A. *Gaussian 98*, revision A.5; Gaussian Inc.: Pittsburgh, PA, 1998. (b) Hu, C.-H.; Chong, D. P. In *Encyclopedia of Computational Chemistry*; Schleyer, P. v. R., Ed.; Wiley: New York, 1998; Vol. 1, pp 669–670.

(17) (a) Mulliken, R. S.; Roothaane, C. C. *J. Chem. Rev.* **1947**, *41*, 219. (b) Mulliken, R. S.; Roothaane, C. C. *Tetrahedron* **1959**, *5*, 253.

(18) (a) Lunell, S.; Huang, M.-B. *Chem. Phys. Lett.* **1990**, *168*, 63. (b) Salhi-Benachenhou, N.; Engels, B.; Huang, M.-B.; Lunell, S. *Chem. Phys. Lett.* **1998**, *263*, 53 and references therein. (c) Eriksson, L. A.; Lunell, S.; Boyd, R. J. *J. Am. Chem. Soc.* **1993**, *115*, 6896. (d) Takahashi, O.; Kikuchi, O. *J. Chem. Phys.* **1994**, *100*, 1350.

TABLE 3. Changes in the Principal Structural Parameters^a of Molecular Structures of Olefin Donors upon Oxidation to Their Cation Radicals

	SA → SA ^{•+}		AA → AA ^{•+}	TME ^b → TME ^{•+}
	ΔX-ray	ΔDFT	ΔDFT	ΔDFT
l (Å)	+0.052	+0.066	+0.068	+0.082
a (Å)	−0.035	−0.033	−0.032	−0.027
b (Å)	+0.016	+0.020	+0.016	
b' (Å)	−0.001	+0.005	+0.017	
c (Å)	−0.004	−0.003	+0.018	
d (Å)	−0.012	−0.005	+0.001	
s ^c (Å)	+0.130	+0.102	+0.098	+0.373
φ (deg)	+29.0	+24.1	+20.9	+11.6

^a See Tables 1 and 2 for definitions. ^b TME = tetramethylethylene. ^c The distance between α-hydrogens.

summarized in Table 3 for sesquihomoadamantene (SA) on the basis of X-ray crystallography and density functional theoretical calculations. Table 3 also includes the calculated changes for the isomeric adamantylideneadamantane (AA) together with those of the parent acyclic analogue tetramethylethylene (TME) for comparison.

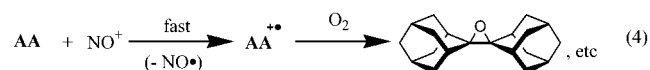
The results in Table 3 show that the cation radicals of the alkyl-substituted ethylenes with rigid (cage) substituents (i.e. SA and AA) and nonrigid substituents (i.e. TME) experience a significant twist around the central olefinic C=C bond. However, the magnitude of the twist varies roughly with the elongation of the olefinic bond, which is greatest (8.2 pm) in the cation radical of tetramethylethylene (TME^{•+}) and is least (6.6 pm) with sesquihomoadamantene (SA). As such, our estimate based on Pauling's bond-distance relationship²³ indicates that the central π-bond order of TME^{•+} (1.28) is less than that of SA^{•+} (1.41), in accord with greater electron delocalization via σ-π hyperconjugation. Therefore, the larger twist in AA^{•+} (20.9°) and SA^{•+} (24.1°) relative to that in TME^{•+} (11.6°) is probably due to other (steric) factors inherent in the rigid bicyclic frameworks. Besides twisting, the acyclic TME^{•+} can relieve nonbonded H···H repulsions (e.g., the closest approach of 1.93 Å in TME, but 2.30 Å in TME^{•+}) by methyl rotation, which is not possible in either AA^{•+} or SA^{•+}. The closest computed H···H separations 1.89 Å in AA and 2.00 Å in SA actually decrease in the planar (*D_{2h}*) conformations of AA^{•+} (to 1.86 Å) and SA^{•+} (to 1.98 Å). Twisting to the *D_{2v}* minima results in substantial elongations to 1.99 and 2.10 Å, respectively. (Note that all these nonbonded separations are still less than the sum of 2.4 Å on the basis of the ideal hydrogen van der Waals radius.) The careful comparison of the bond-length and angular changes accompanying the oxidation of the neutral olefinic donor, as summarized in Table 3, thus shows that the pronounced twist in the cation radical cannot be due to the relief of steric strain. Indeed, the central C=C bond lengthens by 5 pm, which coupled with the other changes in C-C bond lengths leads to an overall enlargement of the annular opening (vide supra) by about 5% in both adamantylideneadamantane and sesquihomoadamantene. The relative steric access to the olefinic chromophores in AA and SA does not experience a dramatic change upon oxidative conversion to their radical cations.

V. Divergent Reactivity of Olefin Donors AA and SA to Electrophiles. Exposure of adamantylideneada-

(23) Pauling, L. *Nature of the Chemical Bond*; Cornell: Ithaca, NY, 1960; p 280.

mantane (AA) to a variety of electrophiles such as bromine, sulfonyl chloride, iodine monochloride, *m*-chloroperbenzoic acid, oxygen, and so forth leads to typical olefin-addition reactions, albeit sometimes at somewhat attenuated rates.^{24–28} On the other hand, when sesquihomoadamantene (SA) is treated with the same electrophiles under identical reaction conditions, no change is observed, even after prolonged periods of exposure. There are however three notable exceptions. Thus, various protonic acids (HX), nitrosonium (NO⁺), and chlorine (Cl₂) react with SA as well as AA in unique ways that shed considerable light on the nature of olefin reactivity. Accordingly, we examined each of these rather small electrophilic reagents with an eye toward understanding the different reaction pathways.

A. Nitrosonium Oxidations to Olefin Cation Radicals. Nitrosonium (NO⁺) usually acts as an electrophilic reagent capable of readily forming carbocationic intermediates by an initial addition of NO⁺ to alkene and arene donors.²⁹ However, nitrosonium reacted rapidly with adamantylideneadamantane via electron transfer to afford the cation radical AA^{•+} in high yields.³⁰ When the reaction was carried out in the presence of dioxygen, AA^{•+} was intercepted by rapid oxygen transfer to afford the epoxide as the basis for an efficient catalytic process.³¹



Sesquihomoadamantene and NO⁺ reacted with similar speed to afford SA^{•+} quantitatively, as described in eq 2. However, the cation radical SA^{•+} was inert to dioxygen, and it persisted unchanged for prolonged periods. Indeed, SA^{•+} is one of the very few carbon-centered radicals that is impervious to dioxygen.

The divergent behaviors of AA^{•+} and SA^{•+} to further reactions of the electrophile can be attributed to differences in thermodynamic driving forces¹¹ as well as steric access of a given reagent to the cation-radical center of the olefinic moiety. Indeed, the van der Waals annulus of 1.6 Å in SA^{•+} is just sufficient to allow only a proton

(24) Bennet, A. J.; Brown, R. S.; McClung, R. E. D.; Klobukowski, M.; Aarts, G. H. M.; Santarsiero, B. D.; Bellucci, G.; Bianchini, R. J. *Am. Chem. Soc.* **1991**, *113*, 8532.

(25) (a) Brown, R. S.; Nagorski, R. W.; Bennet, A. J.; McClung, R. E. D.; Aarts, G. H. M.; Klobukowski, M.; McDonald, R.; Santarsiero, B. D. *J. Am. Chem. Soc.* **1994**, *116*, 2448. (b) Neverov, A. A.; Brown, R. S. *J. Org. Chem.* **1998**, *63*, 5977 and references therein. (c) Wieringa, J. H.; Strating, J.; Wynberg, H. *Tetrahedron Lett.* **1970**, 4579.

(26) (a) Tolstikov, G. A.; Lerman, B. M.; Umanskaya, L. I.; Struchkov, Y. T.; Espenbetov, A. A.; Yanovsky, A. L. *Tetrahedron Lett.* **1980**, *21*, 4189. (b) Huang, X.; Batchelor, R. J.; Einstein, F. W. B.; Bennet, A. J. *J. Org. Chem.* **1994**, *59*, 7108. (c) Garratt, D. J. *Tetrahedron Lett.* **1978**, 1915.

(27) (a) Nelsen, S. F.; Akaba, R. *J. Am. Chem. Soc.* **1981**, *103*, 2096. (b) Akaba, R.; Sakuragi, H.; Tokumaru, K. *Chem. Lett.* **1984**, 1677. (c) Okada, K.; Saito, Y.; Oda, M. *J. Chem. Soc., Chem. Commun.* **1992**, 1731.

(28) (a) Schaap, A. P.; Faler, G. R. *J. Am. Chem. Soc.* **1973**, *95*, 3381. (b) Gill, G. B.; Hands, D. *Tetrahedron Lett.* **1971**, 181. (c) Meijer, E. W.; Wynberg, H. *J. Chem. Educ.* **1982**, *59*, 1071. (d) Clennan, E. L.; Simmons, W.; Almgren, C. W. *J. Am. Chem. Soc.* **1981**, *103*, 2098. (e) Abu-Yousef, I. A.; Harpp, D. N. *J. Org. Chem.* **1997**, *62*, 8366.

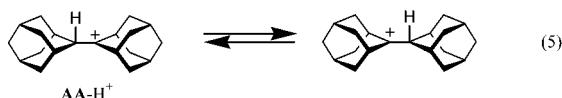
(29) Bosch, E.; Kochi, J. K. *Res. Chem. Intermed.* **1996**, *22*, 209.

(30) Bosch, E.; Kochi, J. K. *J. Am. Chem. Soc.* **1996**, *118*, 1319.

(31) For a review, see: Nelsen, S. F. In *Electron Transfer in Chemistry*; Balzani, V., Ed.; VCH: New York, 2001; Vol. 1, p 342 ff.

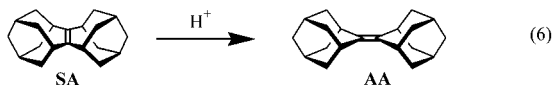
to enter.³² Accordingly, we next turn our attention to the comparative behavior of Brønsted acids toward **AA** and **SA**.

B. Proton Transfer to the Olefin (C=C) Bond. A prechilled solution of adamantylideneadamantane in dichloromethane was mixed with trifluoromethanesulfonic acid at $-10\text{ }^{\circ}\text{C}$ under an argon atmosphere. NMR analysis of the colorless acidic solution at $-30\text{ }^{\circ}\text{C}$ showed characteristic resonances at δ 208.4, 48.7, 44.7, 35.2, and 27.6 in the ^{13}C NMR spectrum due to the protonated **AA**– H^+ .³³ After neutralization with saturated aqueous bicarbonate, quantitative GC and GC–MS analyses of the crude reaction mixture using the internal standard method showed that the neutral donor **AA** was recovered in 98% yield together with traces of unidentified products. These observations are consistent with the earlier NMR investigation by Olah and co-workers³³ in which proton transfer was ascribed to a pair of rapidly equilibrating nonbridged carbocations on the NMR time scale, that is,



The protonated **AA**– H^+ is remarkably persistent, sufficient for the neutral olefin to be recovered quantitatively by simple treatment with aqueous sodium bicarbonate.

The exposure of the isomeric sesquihomoadamantene (**SA**) to strong acids (sulfuric acid, trifluoromethanesulfonic acid, fluorosulfonic acid, etc.) in dichloromethane at $-78\text{ }^{\circ}\text{C}$ led to the rapid and quantitative isomerization to adamantylideneadamantane (**AA**), that is,



The isomerization in eq 6 can also be effected with weaker acids (such as methanesulfonic acid and trifluoroacetic acid), however only at room temperature and after prolonged stirring, as described in Table 4.

The spectral examination of the reaction mixture gave no indication that any cation radical **SA**^{•+} was produced during the isomerization of **SA** in eq 6. Hence, proton transfer to the olefinic carbon center must occur in a single step, since control experiments established that **SA**^{•+}, if it were an intermediate, could have persisted under the acidic conditions. Unlike **AA**, the conjugate acid of **SA** was unstable and rapidly rearranged to that of **AA** via successive Wagner–Meerwein shifts.³⁴

The driving force for such a facile (C–C) rearrangement is consonant with the 10.7 kcal/mol greater ground-state DFT energy for **SA** which may be attributed to the strain of its seven-membered rings. Indeed, the same B3LYP/6-31G* computations show that the initial protonated forms of **A**– H^+ and of **SA**– H^+ both favor classical

TABLE 4. Acid-Catalyzed Isomerization of Sesquihomoadamantene (**SA**) to Adamantylideneadamantane (**AA**) in Dichloromethane^a

acid	temp ($^{\circ}\text{C}$)	time	AA/SA ^b	yield ^c (%)
$\text{CF}_3\text{SO}_3\text{H}$	-10	<1 min	100:0	98
	-78	~10 min	100:0	98
FSO_3H	-78	~10 min	100:0	97
	-10	~10 min	100:0	98
H_2SO_4	-10	~10 min	100:0	98
	$+25$	<1 min	100:0	96
$\text{CH}_3\text{SO}_3\text{H}$	-10	~10 min	100:0	98
CF_3COOH	-10	~10 min	0:100	99
	$+25$	3 h	2:98	98
	$+25^d$	3 h	98:2	96

^a A 5-mL aliquot of a 0.015 M solution of **SA** in CH_2Cl_2 mixed with 1 mmol of acid. For a workup procedure, see Experimental Section. ^b The ratio of the products determined by GC and GC–MS analyses of the crude reaction mixture using an internal standard method. ^c Yield given as total of **SA** and **AA**. ^d Reaction carried out in neat CF_3COOH .

twisted (C_1 point group) structures with **AA**– H^+ being 9.2 kcal/mol more stable (i.e. about the same difference as that between **AA** and **SA** themselves). As a consequence, the (gas phase) proton affinities (to give the most stable **AA**– H^+ and **SA**– H^+ forms) are computed to be nearly the same, 227.9 and 228.9 kcal/mol, respectively. Hence, there is no significant difference in the Brønsted basicities of the two olefins.

The nonclassical, symmetrically bridged (C_{2v} point group) geometries of **AA**– H^+ and **SA**– H^+ represent the transition states for the degenerate proton migration (illustrated for **AA** in eq 5). The isomerization barriers of 9.6 kcal/mol for **AA**– H^+ and 10.7 kcal/mol for **SA**– H^+ reflect the relief of steric strain of the classical forms upon twisting. The twisting effect is shown directly by the energy of classical, untwisted **SA**– H^+ , computed by imposing C_s symmetry, which is only 2.9 kcal/mol lower in energy than the (C_{2v}) transition state but 7.8 kcal/mol less stable than the twisted form.

C. Chlorination of the Olefin Donors **AA and **SA**.** Electrophilic chloronium (Cl^+) transfer to adamantylideneadamantane was readily effected by selective chlorinating agents such as antimony pentachloride and sulfuryl chloride at low temperatures.³⁵ X-ray crystallographic analysis of adamantylideneadamantane chloronium cation (**AA**– Cl^+) established its symmetrically bridged structure **1** in the dihydrotrichloride salt **AA**– $\text{Cl}^+\text{H}_2\text{Cl}_3^-$ produced from SO_2Cl_2 at $-78\text{ }^{\circ}\text{C}$ (Figure 1). However, this structure was easily perturbed to the quasi-bridged structure **2** in the hexachloroantimonate salt **AA**– $\text{Cl}^+\text{SbCl}_6^-$ produced from SbCl_5 at higher temperatures, as depicted in Chart S1 (see Supporting Information).^{35,36} Despite the slight structural variations in **1** and **2**, the crystallographic structures strongly support direct chloronium transfer to the olefinic center of adamantylideneadamantane from both SO_2Cl_2 and SbCl_5 . Furthermore, the addition of **AA** to a colored (yellow) solution of dichlorine in dichloromethane at $-30\text{ }^{\circ}\text{C}$ rapidly led to bleaching; the reaction mixture afforded multiple products, including the chloronium adduct **1**, as well as a mixture of (poly)chlorinated **AA** derivatives. The

(32) Note that the (initial) steric constraints of a proton are affected by its counterion and/or solvation.

(33) Compare ref 1a with: Rathore, R.; Weigand, U.; Kochi, J. K. *J. Org. Chem.* **1996**, *61*, 5246.

(34) (a) A reviewer has pointed out that Wynberg's synthesis¹⁰ of **SA** by the phosphoric acid catalyzed alcohol dehydration (almost certainly) proceeds *via* the protonated **SA** to stop at the 3:1 (equilibrium) mixture of **AA/SA**. (b) For an analogous isomerization, see: Nelsen, S. F.; Kapp, D. L. *J. Org. Chem.* **1985**, *50*, 1339.

(35) (a) Nugent, W. A. *J. Org. Chem.* **1980**, *45*, 4534. (b) Mori, T.; Rathore, R.; Lindeman, S. V.; Kochi, J. K. *J. Chem. Soc., Chem. Commun.* **1998**, 927.

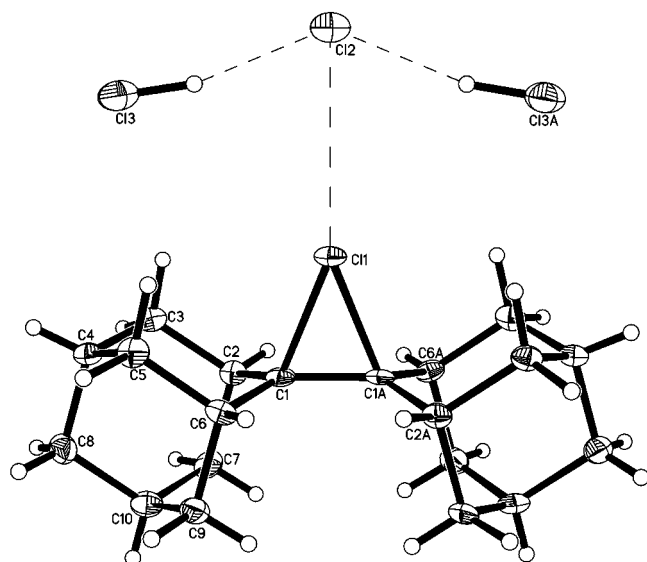
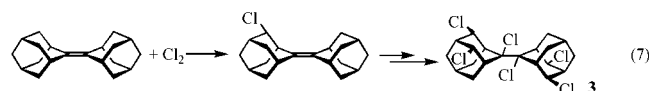


FIGURE 1. ORTEP diagram showing the symmetrical chlorine attachment to **AA** in the adamantylideneadamantanechloronium dihydrotrichloride (**AA**–Cl⁺ H₂Cl₃[–]).

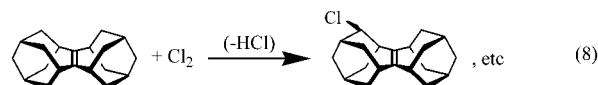
latter were partially elucidated by careful separation of a single crystalline hexachloro derivative **3**. X-ray crystallography unambiguously established only four (equivalent) β -methylene positions in **AA** to be monochlorinated, as shown by the ORTEP diagram (Figure S1 in the Supporting Information) previously reported by Mori et al. in ref 35b. Removal of the solvent from the filtrate revealed the presence of several other unidentified products, most likely consisting of the partial chlorination of the eight β -methylene positions in **AA**, for example,



By way of contrast, chloronium transfer to sesquihomo-

(36) (a) Optimization gave two B3LYP/6-31G* minima for the parent **AA**–Cl⁺ chloronium cation. With *C_s* symmetry, one had a partially bridged geometry; the C–Cl bond lengths 1.940 and 2.197 Å resemble those found in the X-ray structure of the SbCl₆[–] salt. The symmetrical *C_{2v}* minimum (only 0.1 kcal/mol lower in energy) had equal C–Cl bond lengths 2.047 Å (C–C 1.502 Å), which mirror those of the H₂Cl₃[–] salt. Only a *C_s* minimum was computed for the **SA**–Cl⁺ chloronium ion (which was not observed experimentally). However, the symmetrical *C_{2v}* transition structure for movement of the chlorine back and forth was essentially equal in energy. Hence, the actual geometry (with regard to the chlorine placement) of such chloronium ions can be expected to depend on the counterion and the crystal packing. (b) When the chloronium ions from both olefins, **AA**–Cl⁺ and **SA**–Cl⁺, were computed in *C_s* (off-center) and in *C_{2v}* (bridged) symmetry, the energy differences were very small, reflecting flat potential-energy surfaces. However, **AA**–Cl⁺ favored *C_{2v}*, and **SA**–Cl⁺ favored *C_s* symmetry. This behavior is unlike the structural preferences of the corresponding protonated species, **AA**–H⁺ and **SA**–H⁺ (see above). Importantly, the most stable form of **SA**–Cl⁺ is computed to be 21.2 kcal/mol less stable than **AA**–Cl⁺, a difference that exceeds that of the parent olefins, **SA** and **AA**, by 10.5 kcal/mol. Hence, the strain of **SA** would increase greatly upon chlorination, and this fact (a manifestation of the "hyperstability of **SA**")¹¹ could contribute significantly to the difference in behavior from that of **AA**. The epoxides, **AA**–O and **SA**–O, were computed as a further example of possible reaction products. Oxygen is smaller than chlorine, and the local geometries at carbon in epoxides are much like those in the corresponding olefins. Indeed, the energy difference (13.5 kcal/mol) favoring **AA**–O over **SA**–O is only 2.7 kcal/mol larger than the difference between **AA** and **SA**. Consequently, the inertness of **SA** toward epoxidation (in contrast to **AA**) must be ascribed to steric hindrance or other kinetic rather than thermodynamic factors.

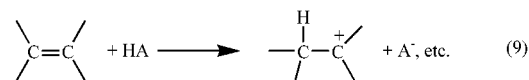
adamantane (**SA**) does not occur with either antimony pentachloride or sulfur chloride, even upon exposure at higher temperatures for prolonged periods. It is also noteworthy that chloronium transfer to the olefinic center of **SA** from dichlorine in dichloromethane at –78° does not lead to an isolable chlorine adduct. Instead, selective *substitution* via chlorination of one or more β -hydrogens occurred, that is,



to yield a chlorinated mixture that was examined by X-ray crystallographic analysis (see Experimental Section). Since spectral analysis during the course of reaction did not detect the cation radical **SA**^{•+}, if it were an intermediate, it must have been highly transient. We conclude that chloronium transfer to the olefinic center of **SA** was not a viable pathway like that observed with adamantylideneadamantane (**AA**).

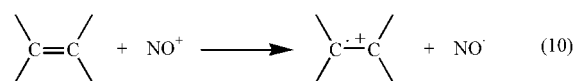
Discussion

X-ray crystallographic analyses and DFT computations establish the structurally related olefinic isomers adamantylideneadamantane (**AA**) and sesquihomoadamantane (**SA**) to differ only slightly (by less than 0.5 Å) in the steric access to the olefinic centers. This is illustrated in Chart 2 that shows the dimensions of the canopies over the olefin centers (provided by four β -protons). Despite this small difference, the olefin reactivities of **AA** and **SA** to electrophilic reagents are strongly differentiated, except with the smallest reagent. For example, proton transfer to the olefinic centers is (more or less) equally rapid to both **AA** and **SA**, the rates generally paralleling the strength of the Brønsted acid (Table 4). The absence of any significant steric differentiation of **AA** and **SA** to proton transfer is in accord with the annular opening in the hydrogenic cavity 2.0 and 1.5 Å which are both large relative to the entering protonic electrophile.³² As such, we conclude that proton transfers directly through the opening to the olefinic carbon centers are most likely to proceed in a single step, that is,



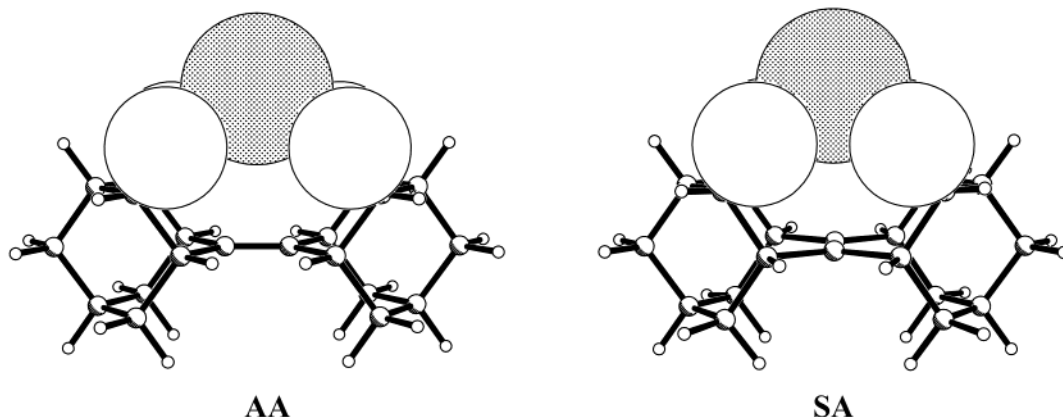
particularly since the cation radical **SA**^{•+} is not an (observable) intermediate in eq 9.

The ease of electron transfer from an olefinic donor to the nitrosonium cation, that is,



is limited by the inner-sphere contact between the C=C center and NO⁺ with van der Waals radii 1.7 and 1.6 Å, respectively.^{37a} In the case of the olefinic donor **SA**, the hydrogenic canopy of four endo β -hydrogens restricts the access to the olefinic center and it precludes the direct

CHART 3

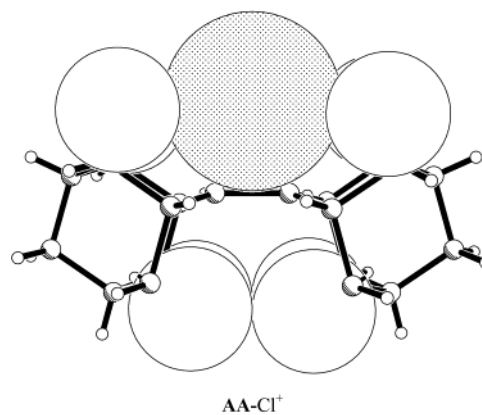


attachment of the electrophilic NO^+ to form a cationic σ -adduct involving a new C–NO bond. The same restriction also applies to **AA**, but to a smaller degree (vide supra). As such, the $>\text{C}=\text{C}</\text{NO}^+$ interaction is limited to an inner-sphere complex in which the separation of NO^+ from the olefinic plane is restricted to a van der Waals contact of 3.25 Å.^{37b} This limitation is graphically depicted as the side perspectives of the inner-sphere complexes of **AA** and **SA** in Chart 3, drawn to scale.^{37d} The large circles represent the limits of the van der Waals radii of the four β -hydrogens, and the shaded circle represents the van der Waals radius of the reactive nitrogen end of the nitrosonium cation that is placed 3.25 Å above the C=C chromophore (for ready visualization).

Chart 3 shows that the annular openings in both **AA** and **SA** are too small to allow penetration of NO^+ into the interior cavity. However, the side perspective (left) in Chart 3 indicates that the annular opening in **AA** is just sufficient to permit the van der Waals contact of NO^+ with the olefinic center, certainly to effect electron transfer, as in eq 10. Moreover, the inner-sphere contact for NO^+ and **SA** shown in Chart 3 (right), although somewhat tight, also falls within the van der Waals limitation for *effective* electron transfer.^{37c} As a consequence, the otherwise electrophilic nitrosonium cation has no choice but to act as a one-electron oxidant.

The comparative (chemical) behavior of **AA** and **SA** toward dichlorine is particularly informative, since only the former leads to the bridged chloronium adduct (**AA**– Cl^+). However, the overall transfer of Cl^+ to **AA** is accompanied by the pyramidalization of both olefin carbon centers (by 16°) to allow the entering Cl to fit into an enlarged cavity at the expense of pushing the four β -protons on the opposite face to within van der Waals

CHART 4



contact, as shown by the side perspective in Chart 4. (Note that the shaded circle represents the van der Waals limit of the bridging chlorine.)

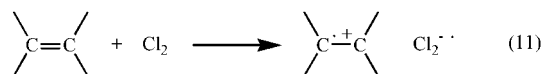
Let us now consider how such a facile “forced” entry of a chlorine atom through the restricted opening of **AA** can occur. Indeed, the appearance of byproducts involving (multiple) chlorinations at the relatively unactivated aliphatic β -methylene positions (described in eqs 7 and 8 and shown by the isolation of the hexachloro derivative **3** in eq 7) suggests that chlorine atoms may be involved as intermediates.³⁸ This conclusion is coupled with the fact that **SA** is not inert but instead reacts with dichlorine to effect an analogous β -chlorination, as in eq 8. The absence of a bridged chloronium adduct (**SA**– Cl^+) is consistent with the restricted annular opening in **SA** plus the fact that pyramidalization of the olefinic centers is much more difficult in **SA** than in **AA**.³⁹ As such, we suggest that an (initial) electron-transfer process via an inner-sphere complex (much like that with NO^+ in eq 10) best accommodates these rather disparate observations,

(37) (a) The importance of the inner-sphere (charge-transfer) complex in electron transfer to NO^+ from various aromatic donors has been discussed by: Rosokha, S. V.; Kochi, J. K. *J. Am. Chem. Soc.* **2001**, *123*, 8985. Compare also: Hubig, S. M.; Rathore, R.; Kochi, J. K. *J. Am. Chem. Soc.* **1999**, *121*, 6170. (b) Preliminary B3LYP/6-31G* DFT computations predict a substantial binding energy of –66 kcal/mol for the analogous olefin charge-transfer complex [**AA**, NO^+]; only a slightly lower energy of –59 kcal/mol applies to the isomeric [**SA**, NO^+] inner-sphere complex, with both manifesting sizable degrees of charge transfer. Their bearing on the distinctive pathways for **AA** and **SA** (described in eqs 4 and 10) will be presented in a separate study. (c) This is not to say (as a reviewer suggests) that electron-transfer cannot take place at greater separations. (d) In Chart 3, the structures are based on the bonding parameters in Table 1, but they may require some modification to those in Table 2 by the extent to which intermolecular charge-transfer pertains.

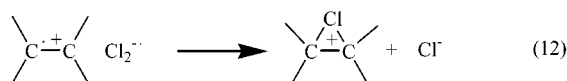
(38) (a) For the facile chain reactions of chlorine atoms and dichlorine leading to aliphatic chlorination, see: Poutsma, M. L. In *Free Radicals*; Kochi, J. K., Ed.; Wiley: New York, 1973; Vol. 2, p 159. Compare also: (b) Fokin, A. A.; Schreiner, P. R.; Schleyer, P. v. R.; Gunchenko, P. A. *J. Org. Chem.* **1998**, *63*, 6494. (c) Fokin, A. A.; Gunchenko, P. A.; Peleshanko, S. A.; Schleyer, P. v. R.; Schreiner, P. R. *Eur. J. Org. Chem.* **1999**, 855, 5. (d) Fokin, A. A.; Schreiner, P. R.; Gunchenko, P. A.; Peleshanko, S. A.; Shubina, T. E.; Isaev, S. D.; Tarasenko, P. V.; Kulik, N. I.; Schiebel, H.-M.; Yurchenko, A. G. *J. Am. Chem. Soc.* **2000**, *122*, 7317.

(39) The formation of the bridged chloronium ion requires an outward and downward bending of the olefinic carbons, which is restrained in **SA** by the pair of rigid bridges.

that is,



Such an electron transfer involving dichlorine has been previously shown with other organic donors,⁴⁰ and it yields an olefin cation radical which is significantly more conformationally flexible⁴¹ to allow chlorine to enter the cavity of **AA** (eq 12), for example,



If so, the subsequent transfer of chlorine in eq 12 most likely proceeds via the prior mesolytic cleavage of the reduced (anionic) dichlorine moiety, that is, $\text{Cl}_2^{\cdot-} \rightarrow \text{Cl}^- + \text{Cl}^\cdot$,⁴² followed by homolytic coupling of the cation-radical/chlorine-atom pair.⁴³

Summary and Conclusion

The variability in the protective (hydrogenic) canopy in the isomeric donors, adamantylenadamantene (**AA**) and sesquihomoadamantene (**SA**), allows olefinic reactivity toward different electrophiles and oxidants to be selectively modulated, **SA** being singularly unreactive except to three sterically limited reagents. Thus, proton transfer to the olefinic center occurs with equal facility to both **AA** (eq 5) and **SA** (eq 6) and the absence of cation-radical intermediates (**SA**^{•+}) strongly indicates that the carbocationic adduct is formed in a single concerted step (eq 9). Moreover, electron transfer from **AA** and **SA** also occurs with equal facility to NO⁺, since the annular openings in their hydrogenic canopies are both sufficient to allow NO⁺ to approach to within a distance requisite to achieve van der Waals' contact for effective inner-

sphere electron transfer (Chart 3).⁴⁶ The different steric requirements of **AA** and **SA** evoke rather unusual reactivity patterns in olefin chlorinations with Cl₂. Thus, the electrophilic transfer of Cl⁺ occurs to afford the bridged chloronium adduct **AA**–Cl⁺, despite the incursion of some skeletal deformations. However, the considerable amounts of chlorination of both **AA** and **SA** at the relatively unactivated aliphatic (β-methylene) positions are attributed to the significant presence of cation radicals (as transient intermediates) that we relate to an initial electron-transfer process (eq 11). As such, “electrophilic” chlorination of olefins is presented as a two-step process involving the prior formation of olefin cation radicals (i.e. eqs 11 and 12).^{43b} In this way, we believe that steric encumbrances and differences in thermodynamic driving force¹¹ in the isomeric donors **AA** and **SA** evoke mechanistic features which are otherwise not so readily apparent with other (less hindered) olefinic donors.

Experimental Section

I. Materials. A mixture of adamantylenadamantane (**AA**) and isomeric sesquihomoadamantene (**SA**) was obtained according to literature procedure^{10,12} and subjected to the standard conditions of epoxidation using *m*-chloroperbenzoic acid in dichloromethane for 1 h at 0 °C. The aqueous workup followed by chromatographic purification on silica gel using hexane as eluent yielded pure sesquihomoadamantene (**SA**) (24%) together with adamantylenadamantane oxide¹⁰ (51%). Recrystallization of both **SA** and **AA** from anhydrous diethyl ether at –30 °C afforded analytically pure samples. Spectral data for **SA**: mp 202–203 °C (lit.¹⁰ mp 199–201 °C); UV–vis (CH₂Cl₂) λ_{max} = 290 nm; ¹H NMR (CDCl₃) δ 1.60–1.90 (m, 20H), 1.98 (m, 4H), 2.12 (m, 4H); ¹³C NMR (CDCl₃) δ 29.3, 35.0, 36.6, 43.5, 149.2. GC–MS *m/z* 268 (M⁺), 268 calcd for C₂₀H₂₈.

Dichloromethane was repeatedly stirred with fresh aliquots of concentrated sulfuric acid (~20 vol %) until the acid layer remained colorless. After separation, it was washed successively with water, aqueous sodium bicarbonate, water, and aqueous sodium chloride, and then dried over anhydrous calcium chloride. The dichloromethane was distilled twice from P₂O₅ under an argon atmosphere and stored in a Schlenk flask equipped with a Teflon valve fitted with Viton O-rings. The hexane and toluene were distilled from P₂O₅ under an argon atmosphere and then refluxed over calcium hydride (~12 h). After distillation from CaH₂, the solvents were stored in the Schlenk flasks under an argon atmosphere.

II. Instrumentation. The UV–vis absorption spectra were recorded on diode array and UV–vis–NIR spectrometers. The ¹H and ¹³C NMR spectra were obtained on a NMR spectrometer. The electrochemical apparatus and the procedures for the determination of oxidation potentials and for the preparation of cation radicals have been described elsewhere.⁴⁷

III. Preparative Isolation of Sesquihomoadamantene Cation-Radical Salt (SA^{•+}SbCl₆[–]). A 100-mL flask equipped with a Schlenk adapter was charged with nitrosonium hexa-

(40) See for example: Eberson, L.; Hartshorn, M. P.; Radner, F.; Persson, O. *J. Chem. Soc., Perkin Trans. 2* **1998**, 59.

(41) The greater torsional flexibility in olefin cation radicals (relative to the parent donor) arises from the (one-electron) depopulation of the bonding HOMO.

(42) Compare: (a) Chupka, W. A.; Berkowitz, J.; Gutman, D. *J. Chem. Phys.* **1971**, 55, 2724. (b) Malone, S. D.; Endicot, J. F. *J. Phys. Chem.* **1972**, 76, 2223.

(43) (a) The competing pathway involving the slight displacement of the chlorine atom within the solvent cage places it adjacent to four (exposed) β-hydrogens to effect the substitutions shown in eqs 7 and 8.⁴⁴ Moreover, chlorine abstraction of a β-hydrogen of the intermediate radical cation could also result in a second intermediate, a homoallylic cation, which would react stereospecifically with chlorine. In effect, the olefin would activate the β-hydrogen positions via a radical cation instead of “onium ion” or cyclopropanoid intermediates.⁴⁵ This mechanism could also result in multiple cation-radical chain chlorinations of the same type that lead to polychlorinated products.^{38a} Radical cation intermediates have been implicated in the substitution and other reactions of saturated cage hydrocarbons without olefinic centers; the regiospecific halogenation of adamantane itself is now believed to proceed via such an electron-transfer mechanism.^{38b–d} (b) We note that the alternative *ionic* mechanism for β-chlorination of **AA** (originally proposed by: Meijer, E. W.; Kellog, R. M.; Wynberg, H. *J. Org. Chem.* **1982**, 47, 2005) is not readily applicable to **SA**, owing to the steric restrictions in the formation of a chloronium adduct. (c) For the equatorial stereochemistry obtained in dichloro derivatives of **AA** from chlorination, see: Nelsen, S. F.; Klein, S. J.; Trieber, D. A.; Ismagilov, R. F.; Powell, D. R. *J. Org. Chem.* **1997**, 62, 6539.

(44) For the ease of homolytic attack of chlorine atoms at unactivated C–H positions, see ref 38a.

(45) See also ref 9b and references therein.

(46) For the quantitative comparison of electrophilic and electron-transfer processes, note that the (DFT) calculated proton affinities and adiabatic ionization potentials of **AA** and **SA** differ by only 1.5 and 2.7 kcal/mol, respectively. For the latter, see also refs 15 and 34b.

(47) Rathore, R.; Kim, J. S.; Kochi, J. K. *J. Chem. Soc., Perkin Trans. 1* **1994**, 2675.

chloroantimonate (73.0 mg, 0.2 mmol), and a chilled (-78°C) solution of **SA** (53.6 mg, 0.2 mmol) in dichloromethane (20 mL) was added under an argon atmosphere. The heterogeneous mixture immediately took on a purple coloration which intensified with time. The highly colored mixture was stirred for 1 h to yield a dark purple solution of $\text{SA}^+\text{SbCl}_6^-$ [λ_{max} (nm) = 360, 485 nm]. This solution was carefully layered with cold hexane (30 mL) and stored in a cold bath at -78°C for 24 h. After this time lapse, the dark red (microcrystalline) precipitate was formed. The dark colored precipitate was quickly filtered under an argon atmosphere, washed with cold hexane (2×10 mL), and dried in vacuo at -50°C for 6 h. The cation-radical salt $\text{SA}^+\text{SbCl}_6^-$ (99 mg, 82%) was stored at -78°C .

The purity of the isolated cation radical $\text{SA}^+\text{SbCl}_6^-$ was determined by iodometric titration, as follows. A solution of $\text{SA}^+\text{SbCl}_6^-$ (63 mg, 0.105 mmol) in cold dichloromethane (20 mL) was added to a solution containing excess tetra-*n*-butylammonium iodide (370 mg, 1 mmol) in dichloromethane (5 mL) at -78°C , under an argon atmosphere, to afford a dark brown solution. The mixture was stirred for 5 min and was titrated (with rapid stirring) by a slow addition of a standard aqueous sodium thiosulfate solution (0.01 M) in the presence of a starch solution as an internal indicator. On the basis of the amount of thiosulfate solution consumed (26.3 mL), the purity of the cation radical was determined to be $>97\%$. With the same procedure, the cation-radical content was also estimated to be greater than $\sim 95\%$ in an electrochemical experiment (vide supra).

IV. Oxidation of Various Organic Donors Using $\text{SA}^+\text{SbCl}_6^-$. The identity of the isolated cation radical SA^+ is further confirmed by its ready ability to quantitatively oxidize a variety of electron-rich organic donors⁴⁸ to the corresponding cation radicals. For example, a 0.21 mM solution of $\text{SA}^+\text{SbCl}_6^-$ (λ_{max} = 360 and 485 nm; ϵ = 4000 and $200\text{ M}^{-1}\text{ cm}^{-1}$) in anhydrous dichloromethane (3 mL) under an argon atmosphere at -78°C was transferred to a 1-cm quartz cuvette equipped with a Schlenk adapter and a side arm which contained the solution of the hydroquinone ether **CRET** (1.1 equiv).⁴⁹ When the two cold solutions were mixed, the reaction mixture immediately turned bright green and the UV-vis spectral analysis confirmed the formation of CRET^+ (λ_{max} = 518 and 486 nm; ϵ_{518} = $7300\text{ M}^{-1}\text{ cm}^{-1}$).³⁷ In a similar manner, a variety of other electron-rich donors with $E^{\circ}_{\text{ox}} < 1.35\text{ V}$ versus SCE were oxidized quantitatively with SA^+ , and the spectra of the donor cation radicals were identical to those obtained by oxidation with either chloranil/methanesulfonic acid⁸ or triethyloxonium hexachloroantimonate.⁵⁰

V. Isomerization of Sesquihomoadamantene (SA) with Brønsted (Protic) Acids. To a cold (-78°C) solution of **SA** (20 mg) in dichloromethane (10 mL) was added 0.1 mL of trifluoromethanesulfonic acid at once. The resulting mixture was stirred for 10 min at -78°C , and the reaction was quenched (rapidly) with saturated aqueous sodium bicarbonate (10 mL). The organic layer was separated, and the aqueous layer was extracted with dichloromethane (2×20 mL). The combined organic layer was dried with magnesium sulfate and evaporated to afford 19 mg of pure adamantylideneadamantane (**AA**), as confirmed by GC, GC-MS, and NMR spectroscopy. A similar procedure was employed for the isomerization of **SA** with other acids (see Table 4).

The cation radical SA^+PF_6^- is stable in a mixture of CH_2Cl_2 (3 mL) and $\text{CF}_3\text{SO}_3\text{H}$ (0.3 mL) at -30°C for at least 30 min. Workup of the reaction mixture by stirring the solution with solid sodium carbonate followed by tetra-*n*-butylammonium iodide yielded neutral **SA** ($\sim 85\%$) together with **AA** ($\sim 5\%$).

A solution of **AA** (10 mg) in dichloromethane- d_2 (1 mL) was treated quickly with 0.1 mL of trifluoromethanesulfonic acid at -30°C , and the NMR spectra were recorded.

VI. Isolation of the Crystalline Salt of the Symmetrically Bridged Chloronium Adduct 2. Adamantylideneadamantane (102.5 mg, 0.16 mmol) was dissolved in 10 mL of dichloromethane at -78°C under an argon atmosphere. Sulfuryl chloride (50 mg, 0.37 mmol) was added with vigorous stirring under a reverse argon flow, whereupon the solution turned blue green. Cold hexane (30 mL) was carefully topped onto the surface of the dichloromethane solution, and the mixture was maintained at -80°C for 15 days. The hydrogen chloride moiety in the crystalline salt was probably due to adventitious water.

VII. X-ray Crystallography. The intensity data for all the compounds were collected with the aid of a diffractometer equipped with a CCD detector using Mo $K\alpha$ radiation (λ = 0.71073 \AA), at -150°C unless otherwise specified. The structures were solved by direct methods⁵¹ and refined by a full matrix least-squares procedure with computers. The details of the X-ray structures described in the Supporting Information are on deposit and can be obtained from Cambridge Crystallographic Data Center, U.K.

VIII. Computational Methods. Density functional theory at the B3LYP/6-31G* level, as implemented in the Gaussian-98 program and detailed in the Supporting Information, was employed for the geometry optimizations, since the structures can be expected to be quite accurate.²² Vibrational frequency computations established the stationary points as minima or as transition structures. In the latter cases, the symmetries were reduced, the geometries were reoptimized, and the frequencies were rerun. The zero point energies (ZPE) were applied uncorrected to the energy evaluations.

IX. Reaction of Sesquihomoadamantene (SA) and Adamantylideneadamantane (AA) with Dichlorine (Cl_2). To a solution of sesquihomoadamantene (**SA**) (200 mg, 0.75 mmol) in dichloromethane (20 mL) at -30°C was added a solution of dichlorine (2 mmol). The pale yellow mixture was stirred for 1 h and evaporated to dryness in vacuo. The resulting (colorless) crude solid (252 mg) contained a mixture of unidentified products together with unreacted **SA**. Note that this white solid readily dissolved in most common organic solvents such as dichloromethane, chloroform, ether, and so forth. Recrystallization of the crude solid from diethyl ether at -30°C afforded single well-formed (visually) colorless crystals. An X-ray examination of the crystals revealed that they were quite similar to crystals of pure **SA** studied earlier. However, the diffraction quality of these crystals was unexpectedly low (absence of high-angle diffractions), and the cell dimensions were systematically larger than those of the pure compound [e.g., at -150°C , a = $6.634(1)\text{ \AA}$, b = $12.091(1)\text{ \AA}$, c = $9.658(1)\text{ \AA}$, β = $90.140(4)^{\circ}$, V = $774.7(4)\text{ \AA}^3$, which represents a cell volume that is 4.5% larger than that of pure **SA**]. X-ray structural analysis resulted in a structure identical to **SA** but with very large thermal displacement parameters and with some large uncompensated peaks of electron density in the difference Fourier maps. These peaks were found at a distance of 1.76 \AA from the β -carbons (although it gave some unreliable intermolecular contacts) and were successfully refined as chlorine atoms with population coefficients of about 4%. The best trial model included four (out of a total of eight) *exo*- β -hydrogens in the **SA** molecule partially substituted by chlorines and gave an *R*-factor close to 0.11. On the basis of the X-ray structural results, we consider the anomalous crystals of **SA** obtained from the chlorination mixture to be a solid solution ($\sim 4\text{ mol \%}$) of β -chlorinated products within the effectively disordered crystalline matrix of the **SA** itself. Unfortunately, the severe disorder in the crystal precluded the determination of accurate molecular structures of the chlori-

(48) For a list of donors that readily form stable cation-radical salts, see ref 8.

(49) Rathore, R.; Kochi, J. K. *J. Org. Chem.* **1995**, *60*, 4399.

(50) Rathore, R.; Kumar, A. S.; Lindeman, S. V.; Kochi, J. K. *J. Org. Chem.* **1998**, *63*, 5847.

(51) Sheldrick, G. M. *SHELXS-86, Program for Structure Solution*; University of Göttingen: Germany, 1986.

nated **SA**. Adamantylideneadamantane (**AA**) was added to a solution of dichlorine in CH_2Cl_2 at $-30\text{ }^\circ\text{C}$, and the resulting pale yellow solution was layered with prechilled ($-30\text{ }^\circ\text{C}$) hexane. A well-formed crop of crystals was obtained after a three-day period at $-23\text{ }^\circ\text{C}$ and mounted for X-ray crystallographic analysis.

Acknowledgment. We thank the R. A. Welch Foundation and the National Science Foundation for

financial support in Texas and a reviewer for detailed suggestions.

Supporting Information Available: X-ray crystallographic and computational data of the compounds discussed in the text, Chart S1, and Figure S1. This material is available free of charge via the Internet at <http://pubs.acs.org>.

JO0200724